

Supplemental Information

PIM Kinase Inhibitor AZD1208 Treats MYC-driven Prostate Cancer

Austin N. Kirschner¹, Jie Wang², Riet van der Meer², Philip D. Anderson³, Omar E. Franco-Coronel⁴, Max H. Kushner⁵, Joel H. Everett², Omar Hameed², Erika K. Keeton⁶, Miika Ahdesmaki⁷, Shaun E. Grosskurth⁶, Dennis Huszar⁶, Sarki A. Abdulkadir^{2,8,9}

¹Department of Radiation Oncology, Vanderbilt University Medical Center, Nashville, TN, USA.

²Department of Pathology, Microbiology and Immunology, Vanderbilt University Medical Center, Nashville, TN, USA.

³Department of Biological Sciences, Salisbury University, Salisbury, MD, USA.

⁴Department of Urology, Vanderbilt University Medical Center, Nashville, TN, USA.

⁵Department of Biological Sciences, Vanderbilt University, Nashville, TN, USA.

⁶AstraZeneca, Oncology iMED, Waltham, MA, USA.

⁷AstraZeneca, R&D Information, Macclesfield, Cheshire, UK.

⁸Department of Cancer Biology, Vanderbilt University Medical Center, Nashville, TN, USA.

⁹Currently at Department of Urology, Northwestern University Feinberg School of Medicine, Chicago, IL, USA.

Corresponding author: Sarki A. Abdulkadir, Northwestern University Feinberg School of Medicine, Department of Urology, Robert H. Lurie Medical Research Center Rm 6-113, 303 E Superior St., Chicago IL 60611 Tel: 312-503-5032. Email: sarki.abdulkadir@northwestern.edu.

Running title: PIM kinase inhibitor treats prostate cancer

Keywords: AZD1208, mouse model, Pim kinase, prostate cancer, p53

SUPPLEMENTAL METHODS

Clonogenic assays and cell line irradiation

Myc-CaP cells were a gift from Charles L. Sawyers [1, 2]. Clonogenic assays and irradiation are described in the Supplemental Methods. From a single suspension of cells, 200 Myc-CaP cells were distributed into quadruplicate 10-cm plates and incubated overnight. A Shepherd Cs-137 irradiator was used to irradiate the cells and within 30 min, AZD1208 in DMSO or DMSO alone was added to a final concentration of 0.1% DMSO. Colonies were fixed and stained with crystal violet in 50% methanol:50% water after 14 days of undisturbed incubation. Colonies greater than 1 mm in diameter were counted using imaging software [3], and verified by hand-count.

Surviving fraction was determined by the formula: $SF = \text{colonies counted} / (\text{number of cells plated} \times \text{plating efficiency})$.

Immunoblotting

For immunoblotting, protein was transferred to Hybond-P PVDF membrane (Fisher Scientific, Pittsburgh, PA), blocked for 1 h in 5% milk in Tris-buffered saline pH 7.4 supplemented with 0.1% Tween-20 (Sigma, St. Louis, MO), and incubated overnight at 4°C in primary anti-Pim1 mouse monoclonal antibody 12H8 (Santa Cruz) at 1:1000 dilution or anti-actin goat polyclonal antibody C-11 (Santa Cruz Biotechnologies, Santa Cruz, CA) at 1:1000 dilution in blocking solution. After washing, secondary antibody incubation with either goat anti-mouse-IgG-HRP conjugate (Biorad, Hercules, CA) at 1:3333 dilution or donkey anti-goat-IgG-HRP conjugate at 1:3333 in blocking solution was performed for 1 h at room temperature. Chemiluminescence was stimulated by Western Lightening Plus ECL reagents (Perkin Elmer, Akron, OH) and detected on HyBlot CL Film (Denville Scientific, South Plainfield, NJ).

Tumor allografts and xenografts

Male athymic nude mice (Fox-n1^{nu/nu}, Harlan Sprague Dawley, Indianapolis, IN, USA) were used for implantation of Myc-Cap allografts. A single-cell suspension of Myc-CaP cells (C. Sawyers) or PC3 cells (ATCC) was mixed with Matrigel (BD Biosciences, San Jose, CA), and allografting was performed by injecting subcutaneously 2×10^6 cells in 0.1 mL Matrigel into each hindlimb (just above the knee) for the radiation experiments or into each flank for non-radiation experiments. Grafts were measured by calipers in two orthogonal dimensions and graft volume was determined by the formula: $0.5 \times \text{axis}_{\text{long}} \times \text{axis}_{\text{short}}^2$ [4]. On the last day of drug treatment within 9 hours of drug administration, mouse kidneys with tissue grafts were harvested 3 hours after intraperitoneal injection of 5-bromo-2'-deoxyuridine (BrdU, Sigma-Aldrich, St. Louis, MO) at 50 mg/kg mouse weight, carefully bisected and then fixed overnight in Protocol 10% zinc-formalin (Fisher Scientific, Kalamazoo, MI, USA), then transferred into 70% ethanol in water for tissue processing and paraffin embedding at the Translational Pathology Shared Resource laboratory at Vanderbilt University Medical Center. Sections were stained with H&E and analyzed by light microscopy. Slides were reviewed in a treatment-blinded fashion by a board-certified pathologist O.H. and scored based on the number of abnormal prostate gland foci (PIN).

For DU145 and CWR22Rv1 cell xenografts, 5-7 week old male NCR nude (Taconic, Germantown, NY) or CB17 SCID (Charles River Labs, Wilmington, MA) mice were implanted with DU145 or CWR22Rv1 cells (ATCC) (6×10^6), with matrigel for CWR22Rv1 and PC3 cells, subcutaneously into the flanks. When graft size reached $\sim 150\text{-}200\text{mm}^3$, mice were randomized and treated once daily with either vehicle, 0.5% Methocel E4M (Gallipot, St. Paul,

MN, USA)/0.1% Tween 80, or AZD1208 by oral gavage with 10 mice per group. Docetaxel was dosed at 6 mg/kg once weekly by IV injection.

Immunohistochemistry

This was performed as described [5]. We used the following primary antibodies with Ph 6.0 antigen retrieval: BrdU (mouse, 1:400, 3G26, Santa Cruz Biotechnology, Santa Cruz, CA), cleaved caspase-3 (rabbit, 1:100, Cell Signaling Technology, Beverly, MA), smooth muscle actin (mouse, 1:2000, Sigma-Aldrich, St. Louis, MO), and GFP that is cross-reactive with YFP (rabbit, 1:500, ab6556, Abcam, Cambridge, MA, USA). For mouse antibodies, treated with Mouse On Mouse (M.O.M.) blocking reagent for 1 h at room temperature (1:60, Vector Labs, Burlingame, CA, USA), followed by background blocking and antibody staining.

Retrieval was performed in 10 mmol/L Tris, 1 mmol/L EDTA, pH 9.0 for the following primary antibodies: c-MYC (rabbit, 1:15000 for 72 hours at 4°C, N-262, Santa Cruz Biotechnology), Pim1 (rabbit, 1:100, Cell Signaling), for immunofluorescence GFP that is cross-reactive with YFP (anti-GFP chicken IgY antibody ab13970, 1:1000, Abcam), phospho-Bad-S112 (rabbit, 1:50, Cell Signaling). The reactivity of ab6556 anti-GFP antibody was verified by immunohistochemical staining of positive and negative control slides. Double immunofluorescence staining was performed for primary anti-MYC and anti-Pim1 with secondary FITC-labeled Tyramide Signal Amplification (1:100, Perkin-Elmer).

Quantification of BrdU and cleaved caspase-3 staining was accomplished by counting the number of positive cells and negative cells per high-powered field in the most affected regions of the tissue section. For Myc-CaP cells, at least 12 independent HPFs were examined from 3 independent tumor samples for each category. For Pim1/c-MYC tissue recombination grafts, at

least 5-12 independent HPFs were examined from 3-10 independent tumor samples for each category.

RNA-seq

RNA samples were submitted to BGI (Cambridge, MA, USA) for RNA-sequencing. Bcbio-nextgen (<https://github.com/chapmanb/bcbio-nextgen>) was used for automated high throughput sequencing analysis which included read quality control, alignment to the mouse genome mm10 padded with ERCC RNA spike-in controls (Life Technologies, Grand Island, NY, USA), and quantification of the raw sequence data to Ensembl gene annotation. The following software was utilized within bcbio-nextgen: cutadapt 1.3, fastqc 0.10.1, bowtie2.1.0, tophat 2.0.10, htseq 0.5.4p5, cufflinks2.1.1 and rnaseq 1.1.7 [6-11]. With respect to the ERCC RNA spike-in controls, samples correlated strongly between the two control mixtures providing high confidence for sequencing reproducibility and sensitivity. The sequencing files were submitted as project PRJEB5525 to the European Nucleotide Archive (<http://www.ebi.ac.uk/ena/>).

For DAVID Functional Annotation Clustering, the on-line tools provided at <http://david.abcc.ncifcrf.gov> were used to perform analyses [12-14]. For each statistical comparison, genes were identified that had an absolute value ≥ 1 log₂ fold-change in expression and ≤ 0.05 raw p-value from a Student's T-test for the gene collapsed log₂ (FPKM+1) expression value (Supplemental_Data_MycCaP_Log2_FPKM_RNAseq_Aanalysis.xlsx document). For each test, the statistically significant up-regulated and down-regulated gene sets were ran separately for functional annotation clustering to identify biological processes that are over-represented with directional change. After submitting a gene set list using the official gene symbol, the "Mus musculus" species was selected to identify functional clusters over-represented with directional

change for a given treatment. Results from the functional annotation clustering were exported as tab delimited text files and select results provided.

For GSEA, the GUI provided at <http://www.broadinstitute.org/gsea/index.jsp> was used to perform analysis [15, 16]. A tab delimited .gct and .cls file was generated separately for the gene collapsed $\log_2(\text{FPKM}+1)$ expression data for the in vitro and in vivo Myc-CaP AZD1208 treated versus DMSO and AZD1208 treated versus control, respectively. For each analysis, the .gct, .cls, and .gmt (c2.all.v4.0.symbols.gmt from GeneSigDB website) files were loaded into GSEA [17]. When running GSEA, the following parameters were used: 1000 permutations, treated versus control phenotype labels, true for collapse to gene symbol, gene_set for permutation type, and chip platforms GENE_SYMBOL.chip, Agilent_MouseGenome.chip, Illumina_MusRef8_v1_1.chip, Mouse430A_2.chip, as well as RefSeq_NP_Mouse.chip to capture as many gene symbols as possible. Results were transferred to Excel for parsing and select results provided.

Supplemental Figures

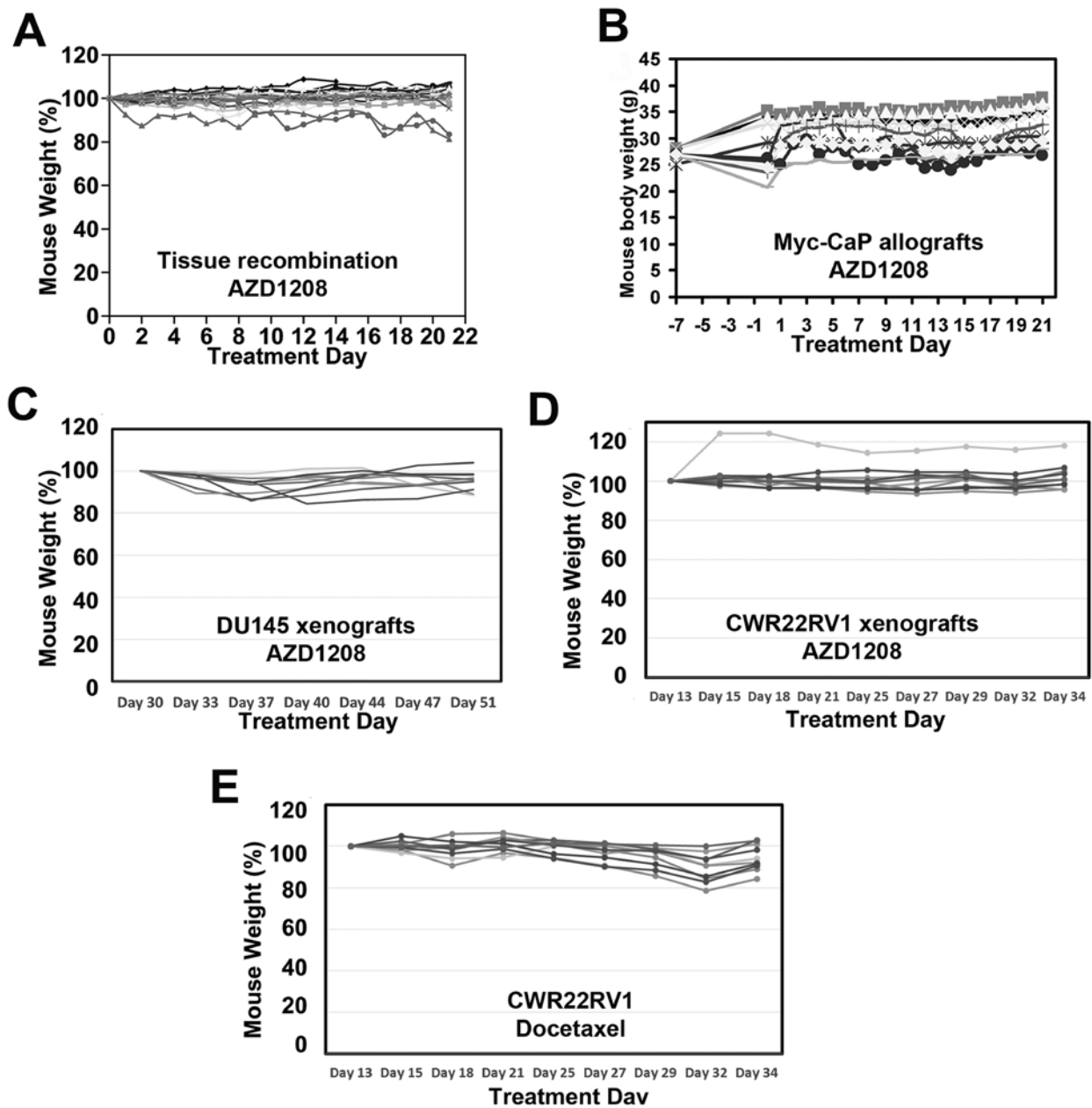


Figure S1. Percent change in mouse weight with AZD1208 or docetaxel treatment. (A) Tissue recombination prostate regeneration experiment. (N=3-6 per group) **(B)** Myc-CaP allograft experiment. (N=6-8 per group) **(C)** DU145 xenograft experiment. (N=10 per group) **(D),** **(E)** CWR22Rv1 experiment. (N=10 per group)

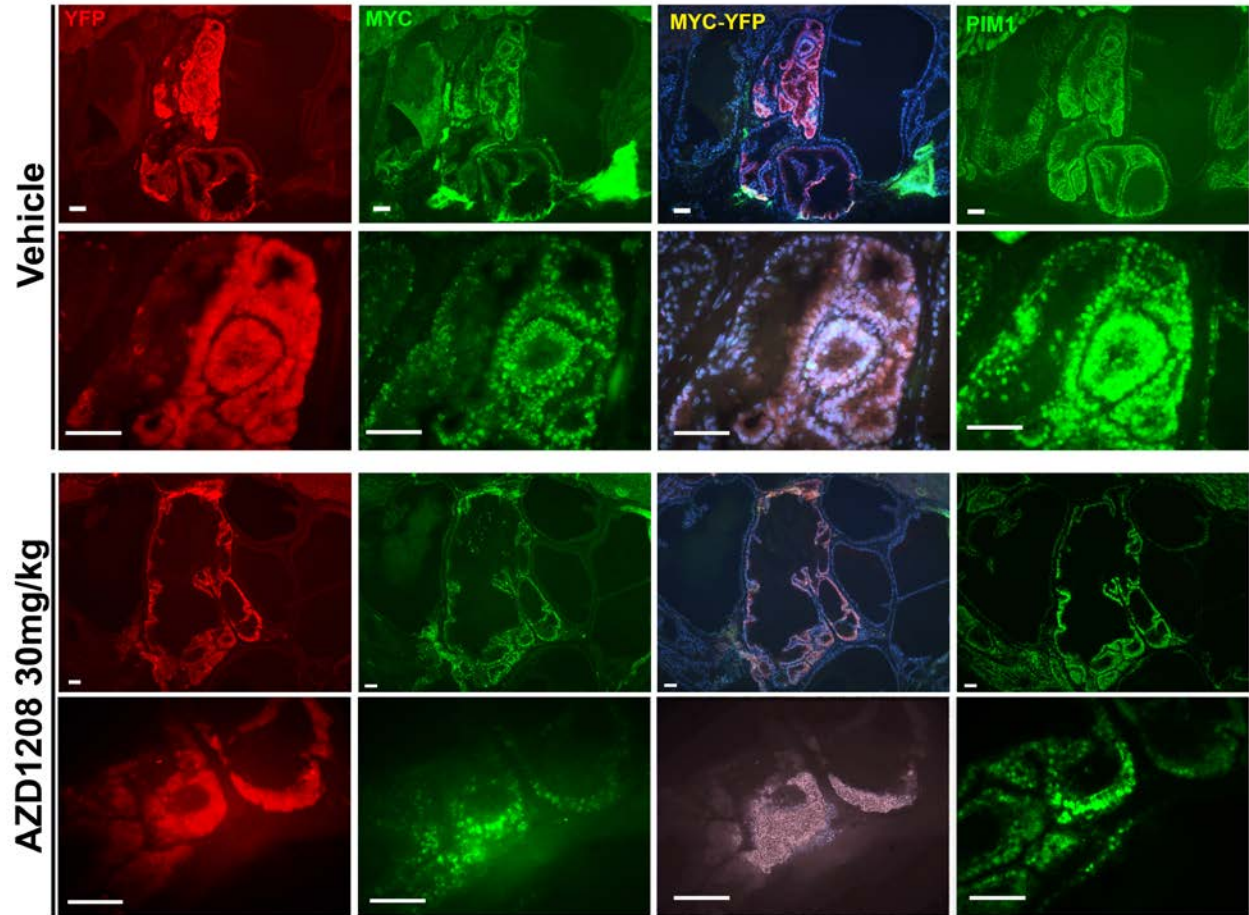


Figure S2. Colocalization of Pim1, MYC, and YFP in prostate grafts. YFP (red), c-MYC (green, 2nd column), and Pim1 (green, 4th column) immunofluorescence in tissue recombination prostate grafts demonstrate co-localization and overexpression of c-MYC and Pim1 for both vehicle-treated and drug-treated specimens (3rd column). 4',6-diamidino-2-phenylindole (DAPI) nuclear stain is blue. Scale bars = 0.05mm.

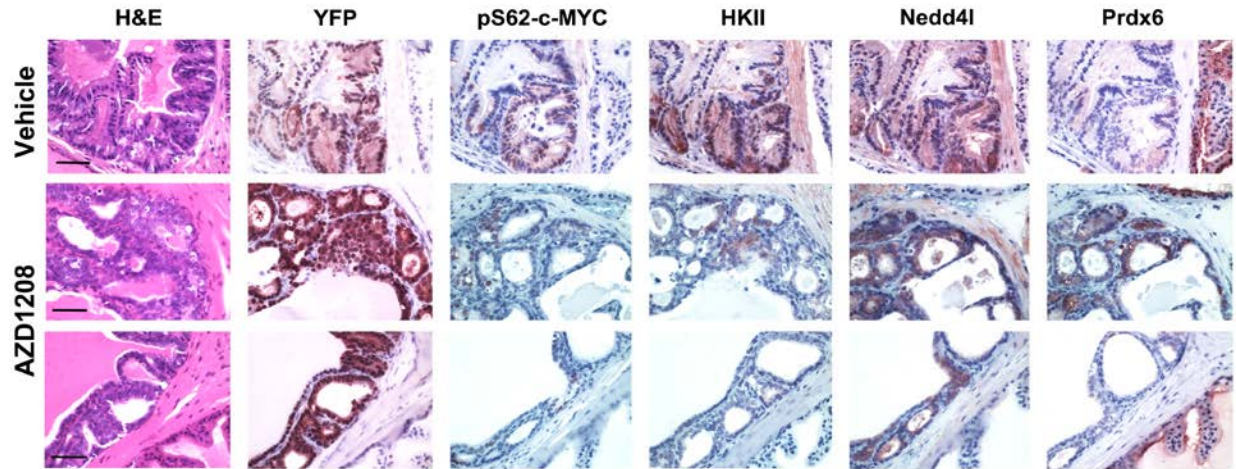


Figure S3. Immunohistochemical stains on tissue recombination prostate grafts for targets related to c-MYC. (A) Adjacent sections stained with H&E and YFP identify abnormal glands (PIN) that express lentiviral c-MYC and Pim1. Pim kinase inhibitor AZD1208 treatment appears to decrease the expression of phospho-S62-c-MYC and hexokinase-II. Scale bars = 0.05mm.

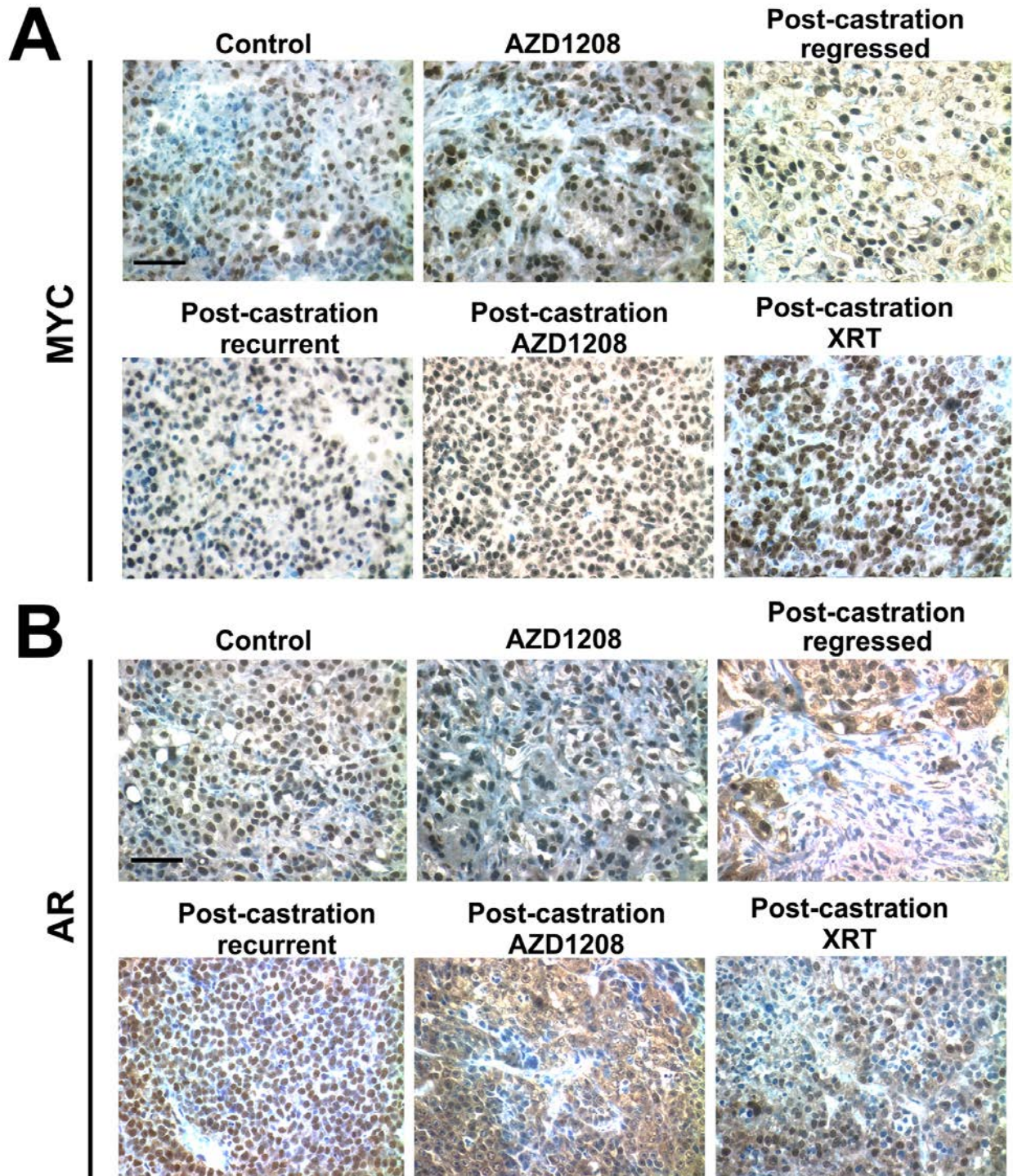


Figure S4. Heterogeneous expression of MYC and AR in regressed Myc-CaP tumors.

(A) MYC immunohistochemistry shows heterogeneous MYC expression in regressed Myc-CaP tumors post-castration. MYC expression is more uniform in tumors from control and AZD1208-

treated mice as well as recurrent tumors in vehicle-, AZD1208- or radiation (XRT)-treated mice.

(B) AR immunohistochemistry reveals heterogeneous nuclear and cytoplasmic expression in regressed tumors after castration. Nuclear AR expression in a more uniform pattern is observed in uncastrated control and AZD1208-treated tumors and in recurrent tumors from vehicle-treated or radiation (XRT)-treated mice. Recurrent tumors in AZD1208-treated mice show nuclear and cytoplasmic AR expression. Scale bar: 50 μ m.

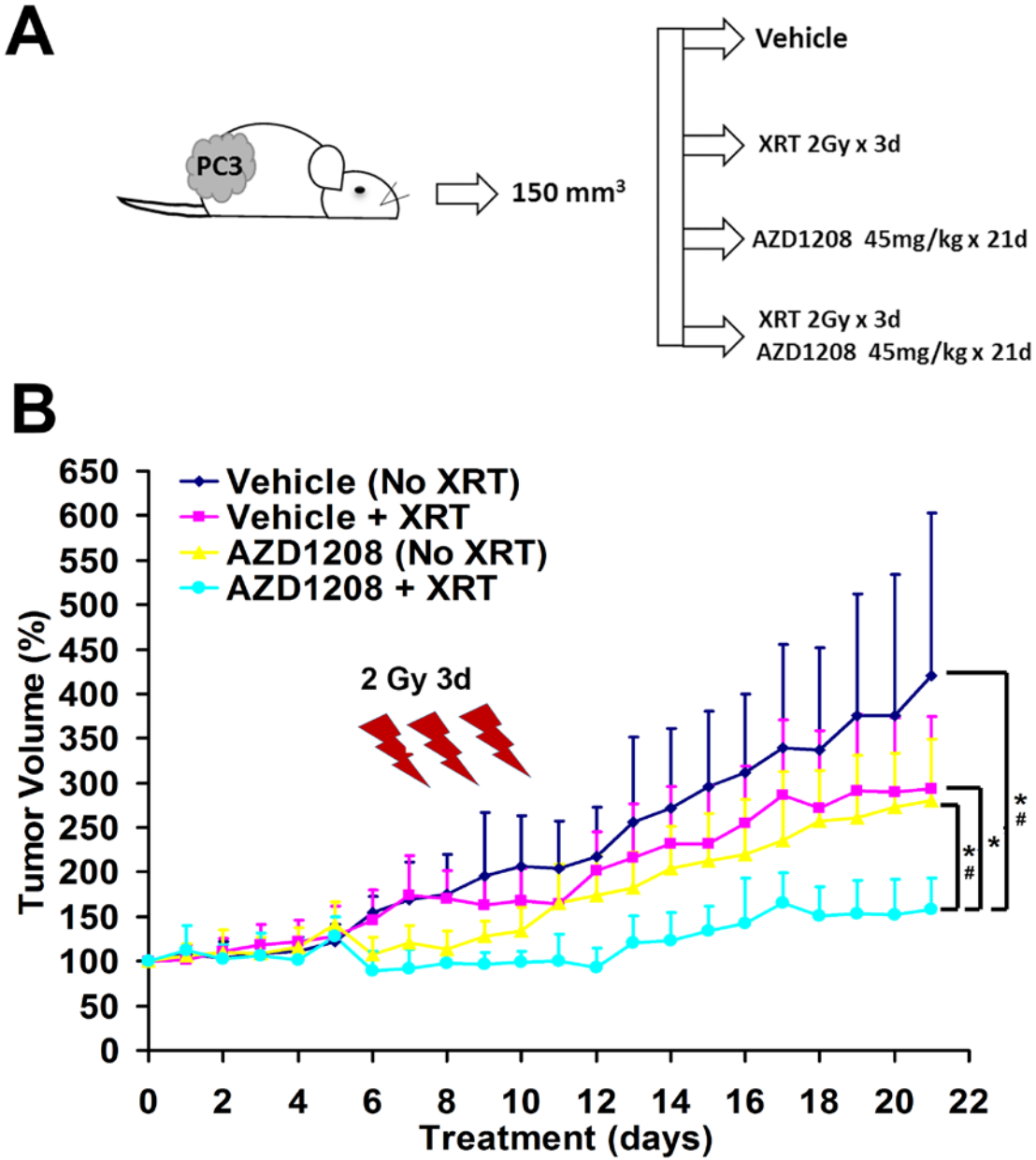


Figure S5. AZD1208 and radiation treatment of human prostate cancer cell line PC3 in xenografts. (A) Schematic of PC3 xenograft experiment and (B) growth curves of PC3

xenografts that were treated with daily with Pim kinase inhibitor AZD1208 at 45 mg/kg or vehicle. Additionally, some mice received 3 daily treatments of 2 Gy of radiation (XRT).

AZD1208-only and radiation-only treated tumors had a delay in growth, but AZD plus radiation

treated tumors show the most sustained inhibition of growth. N=4-6 per group. Results shown as mean \pm SD. *Student's T-test $p < 0.05$. #Mann-Whitney rank sum test significance at < 0.05 .

REFERENCES

1. Ellwood-Yen K, Graeber TG, Wongvipat J, *et al.* Myc-driven murine prostate cancer shares molecular features with human prostate tumors. *Cancer Cell* 2003;4(3):223-38.
2. Watson PA, Ellwood-Yen K, King JC, *et al.* Context-dependent hormone-refractory progression revealed through characterization of a novel murine prostate cancer cell line. *Cancer Res* 2005;65(24):11565-71.
3. Niyazi M, Niyazi I, Belka C. Counting colonies of clonogenic assays by using densitometric software. *Radiat Oncol* 2007;2:4.
4. Yoshida A, Fukazawa M, Ushio H, *et al.* Study of cell kinetics in anaplastic thyroid carcinoma transplanted to nude mice. *J Surg Oncol* 1989;41(1):1-4.
5. Hittelman WN, Liao Y, Wang L, *et al.* Are cancer stem cells radioresistant? *Future Oncol* 2010;6(10):1563-76.
6. Martin M. Cutadapt removes adapter sequences from high-throughput sequencing reads. *EMBnet. journal* 2011;17(1):10-12.
7. Andrews S. FastQC: A quality control tool for high throughput sequence data. 2010; <http://www.bioinformatics.babraham.ac.uk/projects/fastqc/>.
8. Langmead B, Salzberg SL. Fast gapped-read alignment with Bowtie 2. *Nat Methods* 2012;9(4):357-9.
9. Kim D, Pertea G, Trapnell C, *et al.* TopHat2: accurate alignment of transcriptomes in the presence of insertions, deletions and gene fusions. *Genome Biol* 2013;14(4):R36.
10. Anders S, Huber W. Differential expression analysis for sequence count data. *Genome Biol* 2010;11(10):R106.
11. Trapnell C, Roberts A, Goff L, *et al.* Differential gene and transcript expression analysis of RNA-seq experiments with TopHat and Cufflinks. *Nat Protoc* 2012;7(3):562-78.
12. Huang da W, Sherman BT, Lempicki RA. Systematic and integrative analysis of large gene lists using DAVID bioinformatics resources. *Nat Protoc* 2009;4(1):44-57.
13. Huang da W, Sherman BT, Tan Q, *et al.* DAVID Bioinformatics Resources: expanded annotation database and novel algorithms to better extract biology from large gene lists. *Nucleic Acids Res* 2007;35(Web Server issue):W169-75.
14. Huang da W, Sherman BT, Lempicki RA. Bioinformatics enrichment tools: paths toward the comprehensive functional analysis of large gene lists. *Nucleic Acids Res* 2009;37(1):1-13.
15. Mootha VK, Lindgren CM, Eriksson KF, *et al.* PGC-1alpha-responsive genes involved in oxidative phosphorylation are coordinately downregulated in human diabetes. *Nat Genet* 2003;34(3):267-73.
16. Subramanian A, Tamayo P, Mootha VK, *et al.* Gene set enrichment analysis: a knowledge-based approach for interpreting genome-wide expression profiles. *Proc Natl Acad Sci U S A* 2005;102(43):15545-50.

17. Culhane AC, Schroder MS, Sultana R, *et al.* GeneSigDB: a manually curated database and resource for analysis of gene expression signatures. *Nucleic Acids Res* 2012;40(Database issue):D1060-6.